doi: 10.56761/EFRE2024.S3-P-054401

Selection of a receiving antenna for recording high-power microwave radiation

Yu.A. Andreev[1,*], *S.S. Smirnov*[1]

[1]*Institute of High Current Electronics SB RAS, Tomsk, Russia*
[*]*andreev@lhfe.hcei.tsc.ru*

Abstract. By comparison, the effective area A_r of the receiving antenna in the form of the WR-90 waveguide open end in the frequency band 8–12 GHz was determined. An antenna in the form of an open end of a waveguide with a square flange and a pyramidal horn antenna were used as reference. It is shown that the main reason for the resonant nature of the frequency dependence of A_r is reflections from the flange of the receiving antenna. In the work, it was possible to clarify the previously obtained values of A_r.

Keywords: waveguide, pyramidal horn antenna, antenna phase center, effective receiving antenna area.

1. Introduction

High-power microwave sources radiate electromagnetic pulses in the centimeter and millimeter wavelength ranges of nanosecond duration with a power of ~ 10^8–10^9 W [1, 2]. The complexity of measuring the parameters of such microwave pulses is due to: high power level; short duration of the radiation pulse; strong electromagnetic interference created by the switching elements of high-power microwave sources. The measured parameters of the sources include the amplitude, time and energy characteristics of microwave radiation, the radiation pattern and the spectrum.

To register energy in a powerful microwave pulse, calorimetric measurements are used [3] or a directional coupler located on the output horn of the microwave generator. In the second case, it is also possible to obtain the dependence of the generator power over the pulse duration. However, parameters such as the radiation pattern and polarization characteristics of the radiation can only be obtained using antenna measurements. In some studies, the authors try to perform all these measurements in parallel [4]. The thermionic tube diode 6D16D can be used as a detector to register microwave frequencies of centimeter wavelength ranges of gigawatt power level. The sensors consist of a receiving antenna, a waveguide path and a detector section. An open waveguide segment and dipole antennas are usually used as receiving antennas [5], although other options such as a dielectric conical antenna [6] or electric field sensors (D-dot) can be used [7]. With the known sensitivity of the detector, the distance of the sensor from the radiating horn r and the expected power flux density at the receiving point, it is possible to adjust the power coming to the detector only by selecting the effective area of the receiving antenna A_r. Creating of receiving waveguide antennas with the required A_r and the measurement of this parameter in numerical and physical experiments are the purpose of this work.

2. Theory

The receiving antenna A_r was measured using the comparison method (two-antenna method). This technique involves comparing the A_r of the antenna under study and A_{r0} of the reference antenna. The parameters of the reference antenna, if not known before, are measured in the two identical antennas scheme. At the wavelength λ the antenna insertion loss from one antenna to the other P_r/P_t is measured, where P_r is the power at the output of the receiving antenna and P_t is the power at the input to the transmitting antenna. The antennas in the measurement process are located on the same axis and face each other with their apertures facing each other.

The distance between the antenna apertures is R. In addition, the antennas are polarization-matched. In this case, the Friis transmission equation can be written as:

$$\frac{P_r}{P_t} = G_r G_t \cdot \left(\frac{\lambda}{4\pi R}\right)^2, \quad (1)$$

here G_r, G_t – gain coefficients of receiving and transmitting antennas. Equation (1) can also be written for the effective area (aperture):

$$\frac{P_r}{P_t} = A_r A_t \cdot \left(\frac{1}{R\lambda}\right)^2, \quad (2)$$

here A_r, A_t – are the effective areas of the receiving and transmitting antennas. Equations (1, 2) are correctly fulfilled for the far field distance between the antennas:

$$R > \frac{2D^2}{\lambda}, \quad (3)$$

here D is the largest size of any of the antennas.

The effective area of the reference antenna can be found from equation (2) as follows:

$$A_{r0} = R\lambda\sqrt{\frac{P_r}{P_t}}. \quad (4)$$

The effective area of the antenna under the test is found by (2), having previously found A_{r0} by (4).

3. Measurement results

As reference antennas we used the open end of WR-90 waveguide with flange 42×42 mm^2 (Fig.1, position *1*) and a pyramidal horn with aperture 70×92 mm^2 (Fig. 1, position *2*). The height of the horn along its axis is 60 mm. Fig. 2 shows the VSWR dependences on frequency for the two antennas in the form of an open end of a waveguide with a flange, and Fig. 3 VSWR for two pyramidal horns. As can be seen from the above dependencies with high accuracy antennas can be considered identical. The disadvantage of the open end of the waveguide, as it follows from Fig. 2 is a higher VSWR and, consequently, less radiated power. If we take into account that the pattern of that antenna is significantly wider than the pattern of the horn antenna, it becomes clear that the power flux density created by it in the area of the receiving antenna will be significantly less than the horn. However, the open end of the waveguide with a flange has an advantage – the phase center of such an antenna lies in the aperture plane and R in (4) is determined unambiguously.

Fig. 4 shows the experimental and simulated dependences of A_{r0} for the antenna in the form of an open end waveguide with a flange on frequency for R = 25 cm. In the experiment, the dependence of P_r/P_t on frequency was found using an Agilent N5227A network analyzer (provided by shared use center of Tomsk Scientific Center SB RAS) and $A_{r0}(f)$ was calculated using formula (4). Simulations were performed in CST Studio for the same antenna geometry and measurement scheme. Fig.4 shows a good agreement between the simulation and measurement results. The measurements and simulations of $A_{r0}(f)$ were also performed for distances R = 10, 75 and 100 cm. As a result, it is obtained that for $R \geq 25$ cm, $A_{r0}(f)$ changes weakly with increasing R. This indicates that the far zone of the transmitter has been reached. Note that formula (3) gives the calculated value of the far zone R > 24 cm (for the smallest wavelength λ corresponding to the frequency 12 GHz).

Fig. 5 shows the experimental dependences of $A_{r0}(f)$ for the horn antenna on frequency for distances R = 25, 75, 100, 125, and 150 cm. Formula (3) gives the calculated far-field value R > 102 cm for the smallest wavelength λ corresponding to the frequency 12 GHz. As can be seen from Fig. 5, the value of $A_{r0}(f)$ increases with increasing R. This behavior of dependencies can be explained by the fact that the distance R used in the calculation of $A_{r0}(f)$ is the distance between the apertures of horn antennas, not between their phase centers. The phase centers of horn antennas are located on the axis in the direction from the aperture to the input (output) of the horn and are different for *H*- and *E*-planes. We will take a point on the axis with the averaged longitudinal coordinate found for *H*- and

E-planes as phase center of the horn [8]. The dependence of $A_{r0}(f)$ of the horn antenna on frequency, taking into account the distance to the phase centers Δ, is also presented in Fig. 5.

Knowing A_{r0} it is possible to find A_r of the investigated antenna as the open end of the waveguide. The experimental dependences $A_r(f)$ are presented in Fig. 6. The transmitting antenna was an antenna in the form of an open end of the waveguide with a flange. Three receiving antennas with distances from the receiving open end to the flange d = 9.6, 12.9 and 26 cm were investigated. The resulting dependences have a resonant character, determined both by the standing wave between the transmitting and receiving antennas, and by the wave between the inputs of the receiving antennas and their flanges. As can be seen from Fig. 6, the amplitude of the resonances decreases rapidly with increasing d, hence the second mechanism plays a major role in the resonant character of the curves in Fig. 6. In Fig. 6 also shows the $A_r(f)$ dependence obtained with a transmitting horn antenna (d = 9.6 cm for receiving antenna). The data obtained with the two transmitting antennas practically coincide. In addition, Fig. 6 presents the calculated dependence $A_r(f)$ obtained in the numerical experiment in the CST STUDIO. Here, the role of the transmitting antenna was the open end of the waveguide with a flange. The receiving antenna was the open end of the waveguide without a flange.

To keep compact dimensions of the receiving antenna and to get rid of the resonance dependence $A_r(f)$ it is possible to place a rubber absorber on the wide walls of the waveguide (Fig. 1, position *3*). Completely filled with this rubber section of the waveguide length of 10 cm gives an attenuation of 21 dB at a frequency of 9 GHz. In Fig. 7 shows the dependences $A_r(f)$ for a compact receiving antenna (d = 9.6 cm) with an external absorber obtained with the help of transmitting antennas in the form of an open end of the waveguide with a flange and a horn. The dependences $A_r(f)$ obtained in the CST STUDIO environment (similar to Fig. 6) and $A_r(f)$ obtained in [5] for the same receiving antenna are also given here. As can be seen from the above dependences, we managed to obtain a smooth dependence $A_r(f)$ for a compact receiving antenna in the form of an open end of the waveguide and significantly improve the result [5]. To reduce the standing wave in the waveguide of the microwave sensor, a set of attenuators installed along the narrow wall of the waveguide with S21 in the range of 10 - 25 dB are fabricated. By selecting the internal attenuator, the power flux density to the microwave lamp can be additionally adjusted.

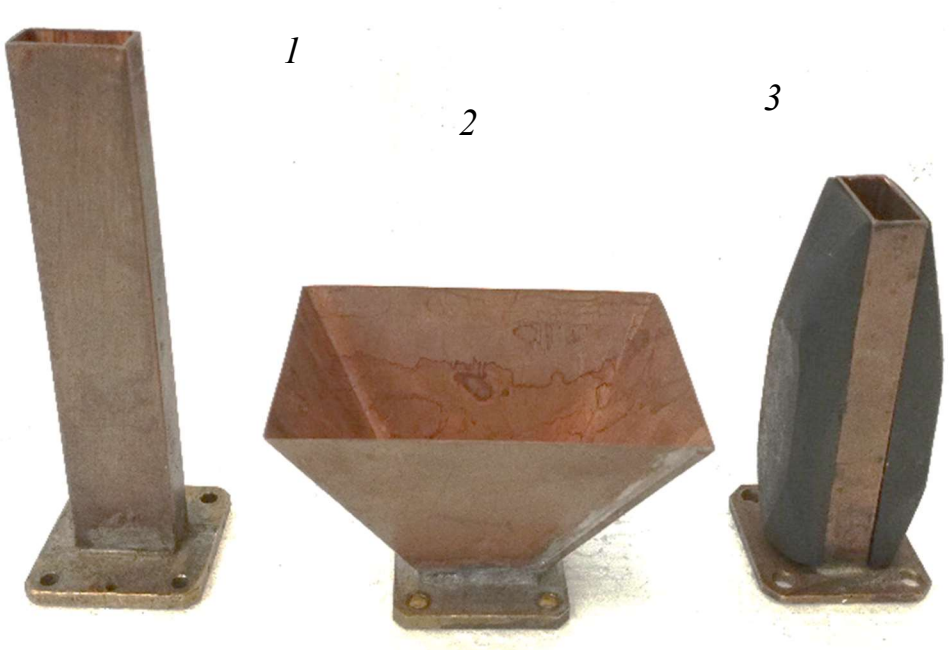

Fig. 1. Antenna in the form of open waveguide end with flange, horn antenna and antenna in the form of open waveguide end with flange and absorbing overlays on the wide walls of the waveguide.

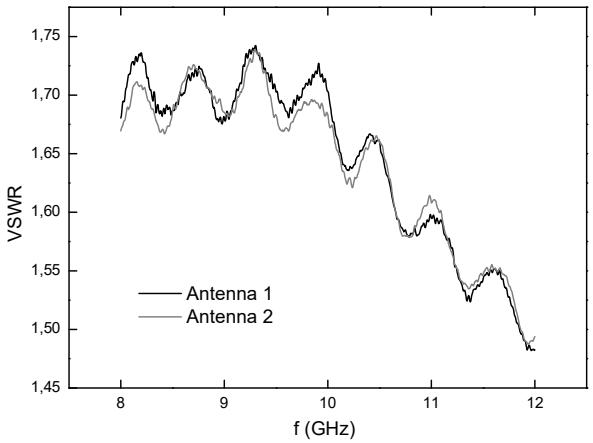

Fig. 2. VSWR dependence for antennas in the form of an open end of a waveguide with a flange on frequency.

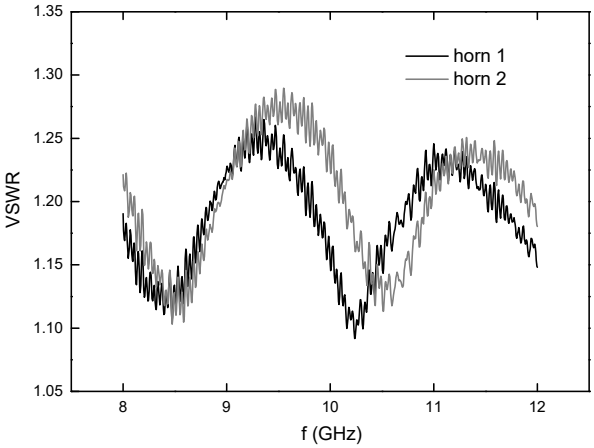

Fig. 3. VSWR dependence of pyramidal horn antennas on frequency.

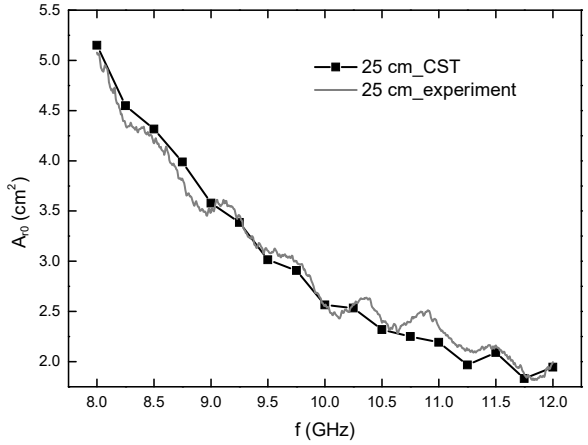

Fig. 4. Experimental and simulated dependences of the effective area of the open end of the flanged waveguide on frequency, measured for R = 25 cm.

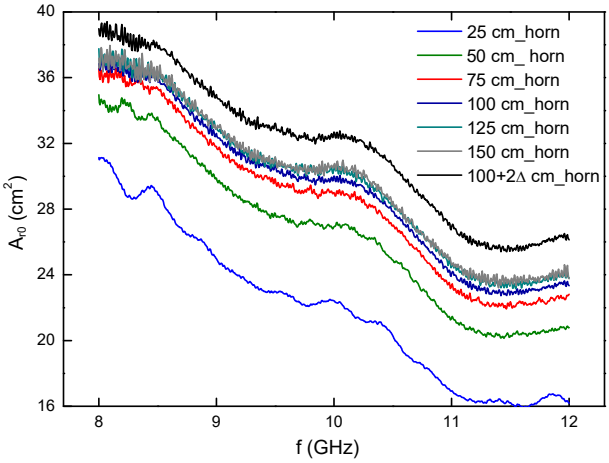

Fig. 5. Experimental dependences of the effective area of the horn on frequency measured for R = 25, 50, 75, 100, 125 and 150 cm.

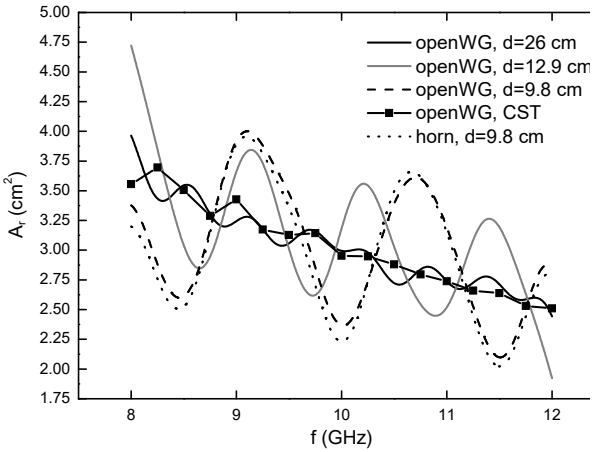

Fig. 6. Experimental dependences of the effective area of the open end of the waveguide on frequency and calculated dependence obtained in CST Studio.

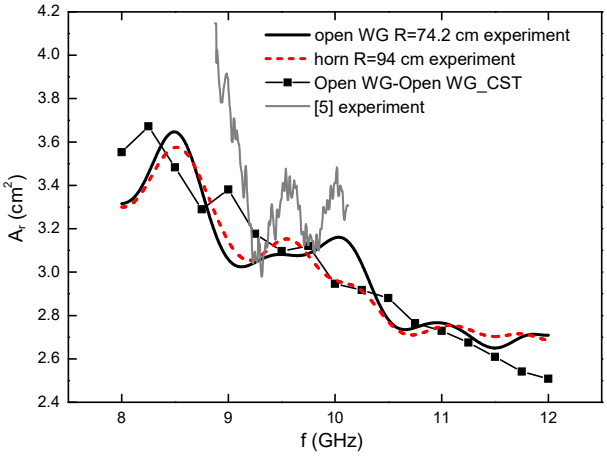

Fig. 7. Experimental $A_r(f)$ dependences for the open end of the waveguide with absorbing overlays and the calculated dependence for the waveguide obtained in CST Studio.

4. Conclusion

In numerical and real experiment measurements of the effective area of the receiving antenna A_r in the form of the open end of the WR-90 waveguide are carried out. The importance of considering the position of the phase center of the horn antenna in finding the A_r of the antenna under study is shown. These antennas have $A_r \approx 3.1$ cm^2 in the frequency band 9–10 GHz, which allows to use them for registration of powerful microwave pulses. In addition to changing the distance from the source, the power flux density to the detector of the receiving antenna can be adjusted by fixed attenuators installed in the waveguide close to its narrow wall. A set of such attenuators with S21 in the range of 10–25 dB is made.

Acknowledgement

The authors express their gratitude to Dr. Vyacheslav Plisko for his help in the work. This work was financially supported by the Ministry of Science and Higher Education of the Russian Federation (Project No. FWRM-2021-0002).

5. References

[1] S. Bugayev, V. Cherepenin, V. Kanavets, A. Klimov, A. Kopenkin, V. Koshelev, V. Popov, A. Slepkov, Relativistic Multiwave Cerenkov Generators, *IEEE Transactions on Plasma Science*, **18**(3), 525, 1990, doi: 10.1109/27.55924

[2] V. Rostov, R. Tsygankov, A. Stepchenko, O. Koval'chuk, K. Sharypov, S. Shunailov, M. Ul'maskulov, and M. Yalandin, High-Efficiency Relativistic Generators of Nanosecond Pulses in the Millimeter-Wavelength Range, *Radiophys. Quantum Electron*., **62**(11), 467, 2020, doi: 10.1007/s11141-020-09992-0

[3] P.V. Vykhodtsev, A.I. Klimov, V.V. Rostov, R.V. Tsygankov and P.V.Priputnev, Wideband Overmoded Liquid Calorimeter for High-Power Microwaves: Centimeters to Millimeters, *IEEE Trans. Instrum. Meas*., **70**, 8001506, 2021, doi: 10.1109/TIM.2020.3034971

[4] Hu Ye, Hui Ning, Wensen Yang, Yanmin Tian, Zhengfeng Xiong, Meng Yang, Feng Yan, and Xinhong Cui, Research on calorimeter for high-power microwave measurements, *Review of Scientific Instruments*, **86**, 124706, 2015, doi: 10.1063/1.4938160

[5] A. Klimov, O. Kovalchuk, V. Rostov, and A. Sinyakov, Measurement of Parameters of X-Band High-Power Microwave Superradiative Pulses, *IEEE Trans. Plasma Sci.*, **36(**3), 2008, doi: 10.1109/TPS.2008.917300

[6] M.R. Ulmaskulov, S.A. Shunailov, K.A. Sharypov, and M.I. Yalandin, Multistage converter of high-voltage subnanosecond pulses based on nonlinear transmission lines, *Journal of Applied Physics*, **126**, 084504, 2019, doi: 10.1063/1.5110438

[7] J.M. Johnson, D.V. Reale, J.T. Krile, R.S. Garcia, W.H. Cravey, A.A. Neuber, J.C. Dickens, and J.J. Mankowski, Characteristics of a four element gyromagnetic nonlinear transmission line array high power microwave source, *Rev. Sci. Instrum.*, **87**, 054704, 2016, doi: 10.1063/1.4947230

[8] C. Balanis, *Antenna theory analysis and design*, *4th ed*. Hoboken, NJ, USA: Wiley, 2016.